

RSC Advances



This is an *Accepted Manuscript*, which has been through the Royal Society of Chemistry peer review process and has been accepted for publication.

Accepted Manuscripts are published online shortly after acceptance, before technical editing, formatting and proof reading. Using this free service, authors can make their results available to the community, in citable form, before we publish the edited article. This *Accepted Manuscript* will be replaced by the edited, formatted and paginated article as soon as this is available.

You can find more information about *Accepted Manuscripts* in the [Information for Authors](#).

Please note that technical editing may introduce minor changes to the text and/or graphics, which may alter content. The journal's standard [Terms & Conditions](#) and the [Ethical guidelines](#) still apply. In no event shall the Royal Society of Chemistry be held responsible for any errors or omissions in this *Accepted Manuscript* or any consequences arising from the use of any information it contains.

Adsorption of toxic acidic dye from aqueous solution onto diethylenetriamine functionalized magnetic glycidyl methacrylate - N,N' methylenebisacrylamide

K.Z. Elwakeel^{*a}, A.A. El-Bindary^b, A.Z. El-Sonbati^b, A.R. Hawas^b

^a Environmental Science Department, Faculty of Science, Port-Said University, Port-Said, Egypt

^b Chemistry Department, faculty of Science, Damietta University, Damietta 34517, Egypt

Abstract

Magnetic sorbent microgranules with magnetite (Fe₃O₄) core and glycidyl methacrylate/ N,N' methylenebisacrylamide shell were prepared (MGMA). Diethylenetriamine (DETA) was successfully grafted (through a relatively simple solution reaction) onto the magnetic microgranules to obtain a sorbent (MGMA-DETA) with a very high content of amine groups. The obtained sorbent (MGMA-DETA) was characterized by Fourier transform infrared (FTIR), scanning electron microscopy (SEM), transmission electron microscopy (TEM), Powder X-ray diffraction (XRD), vibrating sample magnetometer (VSM) and thermogravimetric analysis (TGA). This material showed high affinity for Acid Yellow 99 dye (AY99) uptake from aqueous solutions: maximum sorption capacity reached 0.25 mmol g⁻¹ at pH 3.0 and ambient temperature (i.e., 25 ± 1 °C). Uptake kinetics and sorption isotherms were obtained and modeled using conventional and simple equations: best results were respectively obtained with the pseudo-second order rate equation and the Langmuir equation. The distribution coefficient was obtained at different temperatures and the thermodynamic parameters have been calculated: the sorption is

* Corresponding author: Fax: +20(0)1061694332.
E-mail address: Khalid_elwakeel@yahoo.com (K.Z. Elwakeel).

endothermic, spontaneous (especially at high relative temperature) and contributes to increase the entropy (randomness) of the system. NaOH solution (1.0 M) was used for AY99 desorption from loaded sorbents, and the sorbent could be efficiently recycled for a minimum of three sorption/desorption cycles. Therefore, MGMA-DETA could serve as a promising adsorbent for AY99 removal from industrial wastewater.

Keywords: AY99; Magnetic sorbent; Glycidyl methacrylate; Sorption isotherms; Kinetics; Thermodynamics

1. Introduction

Acid dyes are widely used in various industries such as textiles, paper, leather, and plastics. The presence of such dyes in water bodies may be mutagenic and carcinogenic and can cause severe damage to the liver, digestive and the central nervous system of human beings and affect agricultural cultivation and underground water quality [1]. Wastewater from industries is highly colored and the residual acid dyes in it are seriously concerned for their adverse effects to human beings and the environment [2]. Thus, the removal of dye pollutants from wastewater is necessary and important before colored effluents are discharged into the environment. Nowadays since the legal regulations concerning disposal of colored waste waters into the natural environment are more and more restrictive. Many technologies have been developed for the acid dyes removal from aquatic environment, including physical, chemical and biological approaches [3]. However, most chemical and biological methods with high cost or low degradation efficiency are rarely used in the actual treatment processes [4], some physical sorption approaches also encountered low removing efficiencies of dye [5]. Adsorption of hazardous materials on adsorbent is considered to the most effective method for waste water treatment in terms of cost, ease of operation, flexibility and simplicity of design [6]. Among the numerous types of adsorbents, magnetic particles as adsorbents have opened a new field in separation technology [7]. The application of a magnetic field induces the magnetization of the material and thus makes the use of a magnetic force possible, but when the magnetic field is cut of, the magnetization immediately decreases to zero. It is important for the release of particles after adsorption of the waste. On the other hand, glycidyl methacrylate (GMA) is one of the most studied polymer matrix in modification reactions due its good mechanical strength, acid and alkali resistance, porous

structure, abrasion resistance, high tensile strength, and cheaper cost than any other vinyl based polymers [8,9]. However, the main drawback for this material consists of the difficulty to separate adsorbent particles at the end of the adsorption process due to the difficulty in separating the suspension from aqueous solution by filtration or centrifugation, which may increase the cost of industrial application. This problem can be overcome by incorporating a magnetic core in the GMA particles: an external magnetic field allows recovering the particles at the end of adsorption step [10-13]. The most commonly used magnetic adsorbents are based on Fe_3O_4 particles [14, 15]. Magnetic adsorbents are usually composed of a magnetic core (to ensure a strong magnetic response) and a polymeric shell (to provide selective functional groups) [16,17]. GMA possessing high reactive epoxy groups in the side chain, which makes it very reactive for chemical modification or for reacting with other materials. To prepare amine functionalized GMA based sorbents, numerous studies have been carried out using polyamines such as ethylenediamine (EDA), diethylene triamine (DETA), triethylene tetraamine (TETA) and tetraethylene pentaamine (TEPA). In spite of its high sorption capacity for heavy metals and its versatile properties, rare work is available in the literature about the sorption of dye anions into amine functionalized GMA based sorbents. Therefore, in this study, it is aimed to synthesize a magnetic composite made of glycidyl methacrylate (GMA) (coating the magnetic Fe_3O_4 core) that is functionalized by grafting diethylenetriamine (DETA) through GMA (to increase the density of sorption sites (and their potential selectivity)). Different techniques are used for the physicochemical characterization of the adsorbent, including FTIR spectrometry, scanning electron microscopy (SEM), transmission electron microscopy (TEM), Powder X-ray diffraction (XRD), vibrating sample magnetometer (VSM) and thermogravimetric analysis (TGA). In a second step the

adsorbent is being tested for Acid Yellow 99 dye (AY99) recovery through the study of pH effect, the determination of adsorption isotherms and thermodynamic characteristics and the identification of controlling steps in uptake kinetics, the application for removal of AY99 from polluted effluent will be studied. Finally, desorption of AY99 was studied with the objective of verifying the possibility to recycle the sorbent.

2. Materials and method

2.1. Chemicals and reagents

All chemicals used were of analytical grade and demineralized water was used for the preparation of all aqueous solutions. Glycidyl methacrylate (GMA) was provided by Riedel-de Haën (Germany), while N,N'-methylenebisacrylamide (MBA) and benzoyl peroxide (Bz_2O_2) were supplied by Fluka AG (Switzerland). Diethylenetriamine (DETA) was obtained Sigma-Aldrich (Switzerland) while isopropyl alcohol was provided by Carlo Erba (France). All other chemicals were Prolabo products and were used as received. Acid Yellow 99 was used for the preparation of the stock solution.

Fe_3O_4 particles were synthesized by co-precipitation of ferric and ferrous salts following a procedure derived from the so-called Massart method [18]. The amounts of 6.480 g of $FeCl_3 \cdot 6H_2O$ and 3.334 g of $FeSO_4 \cdot 7H_2O$ were dissolved into 150 mL of demineralized water. Then 2 mL of HCl was added under continuous stirring for 30 min, until complete dissolving of precursor's salts. The chemical precipitation was achieved at 30 °C under vigorous stirring by drop wise addition of 10 mL of NaOH solution (50%, v/v). During the reaction process, pH was maintained around pH 11. The reaction system was maintained under agitation at 30 °C for 15 min. The product was then washed with distilled water several times and stored for use.

2.2. Synthesis of the magnetic-GMA

The magnetic-Glycidyl Methacrylate sorbent was prepared through the polymerization of GMA (9.8 g) in the presence of 3.0 g of magnetite particle. MBA (0.2 g) corresponding to a mass ratio of 2% (referred to GMA amount) was used as a cross-linking agent; 0.1 g of Bz_2O (acting as the initiator of the polymerization reaction) was added under agitation. 3 mL of isopropyl alcohol and 25 mL of cyclohexane were mixed and added to the former solution. The solution was then poured into a flask containing 100 mL (1%) polyvinyl alcohol and heated on a water bath at 75–80°C under continuous stirring for 3 hr. The product was filtered off and washed repeatedly with demineralized water and acetone before being air-dried. The product was called MGMA.

2.3. Diethylenetriamine grafting on MGMA

MGMA (5 g) was suspended in dioxane (100 mL) and then treated with 10 mL of Diethylenetriamine (DETA). The suspension was stirred at 75 °C for 12 h. The product was washed with water followed by acetone. The product was then air-dried, grinded, sieved into fractions <1000 μm and called MGMA-DETA.

2.4. Estimation of the amine content

A titration method was used to estimate the accessible amine contents of MGMA-DETA for metal ion adsorption [7]. A 0.5 g amount of MGMA-DETA was added into 50 mL of 0.05 M HCl solution for 15 hr for the protonation of the amine groups of MGMA-DETA. Then, the protonated MGMA-DETA was separated by a magnetic field and the solution was collected. The initial and final concentrations of HCl in the solution were determined through volumetric titration with 0.05 M standardized NaOH (using phenolphthalein as the titration indicator). The difference in the acid

concentrations was used to calculate the acid capacity of MGMA-DETA. The accessible amine content of MGMA-DETA was then obtained from the assumption that one neutral amine consumed one proton. The concentration of amino group was calculated by the following equation

$$\text{Concentration of } (NH_2) \text{ groups} = \frac{(M_1 - M_2) \times 50}{0.5} \quad (\text{mmol/g resin}) \quad (1)$$

where M_1 and M_2 are the initial and final concentrations of HCl.

2.5. Characterization of MGMA-DETA

In order to confirm the functionalization of the sorbent; magnetite glycidyl methacrylate resin was examined in dried KBr powder by recording the infrared spectrum over the range of 4000–400 cm^{-1} using a Fourier transform infrared (FTIR) spectrophotometer (Jasco FTIR-4100 spectrophotometer). The morphology and the elemental distribution of AY99 in the magnetic sorbent was analyzed with a Scanning Electron Microscope (JEOL JSM 6510 IV). The structure of the synthesized MGMA-DETA was examined by X-ray diffraction measurement (XRD) is recorded on X-ray diffract meter in the range of diffraction angle $2\theta = 5-80^\circ$. This analysis is carried out using $\text{CuK}\alpha 1$ radiation ($\lambda = 1.540598 \text{ \AA}$). The applied voltage and the tube current are 40 KV and 30 mA, respectively. Thermal analysis of the sorbent is carried out using a Shimadzu thermo gravimetric analyzer under nitrogen atmosphere with heating rates of 10-15°C/min over a temperature range from 20.53 °C up to 999.2 °C.

2.6. Sorption experiments

A stock solution ($1 \times 10^{-3} \text{ M}$) of AY99 dye was prepared in distilled water. The other solutions were obtained by dilution of the stock solution with distilled water just prior

experiments. For the study of pH effect 25 mL of 5×10^{-4} M solution at different pH values (in the range 1-9) were mixed with 50 mg of sorbent (dried weight) for 3 h, and the stirring speed was maintained at 40 rpm using a reciprocal agitator, Rota bit, J.P. Selecta (Spain). The pH values were adjusted by addition of 0.1, 0.01 N HCl and 0.1, 0.01 N NaOH solutions and measured by using a pH meter (Aqualytic AL15). Samples were collected and filtrated through magnetic separation and the filtrate was analyzed for residual AY99 concentration using Perkin-Elmer AA800 spectrophotometer (Model AAS) at wavelength of 418 nm. The pH was not controlled during the sorption but the final pH was systematically recorded. The concentration of the released iron during adsorption was analyzed using analyzed using flame atomic absorption spectrophotometer (solar-969, AAS) supplied with acetylene and nitrous oxide burner heads and integrated reading for absorbance.

For sorption isotherms 50 mg of sorbent (m) were mixed with 25 mL (V) of AY99 solutions at different initial concentrations (C_0 , ranging between 8×10^{-5} and 1×10^{-3} M) for 3 h. The pH of the solutions was initially set at 3. After solid/liquid separation, the residual concentration (C_e , mmol AY99 L^{-1}) was determined by a UV-vis spectrophotometer and the sorption capacity (q_e , mmol g^{-1}) was determined by the mass balance equation:

$$q_{eq} = \frac{(C_0 - C_e)V}{m} \quad (1)$$

Where C_0 and C_e is the initial and equilibrium concentration of metal ion in solution (M), respectively, V is the volume of solution (L) and m the mass of sorbent (g).

For uptake kinetics 250 mg of sorbent were mixed with 125 mL of AY99 solutions (C_0 : 5×10^{-4} M) at pH 3. Samples (4 mL) were collected (the sorbent being

magnetically separated) at fixed times and the residual concentrations were determined by UV–vis spectrophotometer. The agitation speed was set at 100 rpm while the temperature was maintained at 25 ± 1 °C. The sorbed amount of AY99 per unit weight of the sorbent at time t ($q(t)$, mmol AY99 g^{-1}), was calculated from the mass balance equation (taking into account the decrement in the volume of the solution) according:

$$q(t) = \sum_{i=1}^n \frac{(C(t)_{(i-1)} - C(t)_{(i)}) \times V(t)_{(i-1)}}{m} \quad (2)$$

where $C(t)_{(i)}$ (M) is the AY99 concentration of the withdrawn sample number i at time t and $C(t)_{(0)} = C_0$, $V(t)_{(i)}$ (mL) is the volume of the solution in the flask at sample number i and time t , and m is the mass of the sorbent in the flask. Here $V(t)_{(i)} - V(t)_{(i-1)}$ equals 4 mL (the sample volume).

The effect of temperature on the adsorption of AY99 was carried out in the 25mL of dye solutions (5×10^{-4} M, pH 3) with 0.05 g of adsorbent for 90 min at various temperatures (20,25,30,35 and 40°C).

The effect of sorbent dose on AY99 dye removal was carried out in the 25 mL of dye solutions (5×10^{-4} M, pH 3) with sorbent mass in the range 0.01- 0.1g of adsorbent at 25 ± 1 °C for 90 min.

The effect of chloride ion on AY99 removal was examined, by addition of increasing concentrations of NaCl (from 5 to 40 $g L^{-1}$; C_0 : 5×10^{-4} M, pH 3; sorbent dosage: 50 mg of sorbent for 25 mL AY99).

Regeneration experiments were performed by contact of 0.5 g of the sorbent with 100 mL of 5×10^{-4} M AY99 at pH 3 for 90 min. The amount of dye sorbed (and the

sorption capacity) was determined by the mass balance equation (Eq. 1). The solution was magnetically decanted and the adsorbent was washed by distilled water. The loaded sorbent was mixed with 25 mL of 1 M NaOH for 30 min. The regenerated sorbent was magnetically decanted, then carefully washed by distilled water for reuse in the second run. The regeneration efficiency (RE, %) was calculated according to the following equation:

$$\text{RE \%} = \frac{\text{Amount of adsorbed AY99 (mmol) at run (n + 1)}}{\text{Amount of adsorbed AY99 (mmol) at run (n)}} \times 100 \quad (3)$$

3. Results and discussions

3.1. Characterizations of synthesized MGMA-DETA

Figure SM1 (see Supplementary Material Section) shows the FTIR spectrum of MGMA-DETA particles for the wavenumber range 4000-400 cm^{-1} . The $>\text{C}=\text{O}$ stretching vibration is observed at 1602.56 cm^{-1} ; the $-\text{C}-\text{O}-$ stretching vibration appears as a shoulder close to the peak observed at 1031.73 cm^{-1} (C-N stretching). The characteristic peak at 907 cm^{-1} , which is assigned to the epoxy group of GMA [19], completely disappeared on the spectrum of MGMA-DETA sorbent: this means that DETA reacted with all epoxy groups present on the support and that the grafting of DETA was successful. The peaks associated to amine groups are observed at 1400.07 cm^{-1} (N-H bending), 1031.73 cm^{-1} (C-N stretching) and 950 cm^{-1} (N-H wagging). All these new and strong peaks confirmed the grafting of numerous amine groups (from DETA) on PGMA backbone. In addition, the broad band centered at 582.39 cm^{-1} is generally assigned to $\gamma\text{-Fe}_2\text{O}_3$ [20], while Fe_3O_4 is reported at 560 cm^{-1} (Fe-O vibration for magnetite support) [21].

The amine content in the sorbent was determined by titration: 3.9 mmol g^{-1} . This also confirms the successful grafting of DETA on the material.

Scanning electron microscope is useful for determining the particle shape and appropriate size of the adsorbent. In addition, it is important tool for characterizing the surface morphology and fundamental physical properties of the adsorbent surface. Figure 1 shows the SEM analyses of the sorbent before and after AY99 adsorption. The surface of the MGMA-DETA is generally smooth, Spherical particles of the MGMA-DETA can be clearly observed, the diameter was in the range of $\approx 0.55 \mu\text{m}$. The microscopic observation of the surface of the MGMA-DETA sorbent particles after AY99 adsorption does not show significant changes in the external structure.

The TEM images of the sorbent are shown in Figure 2: the particles have a spherical and regular morphology and are homogeneously distributed in size. The structure of the sorbents was monodisperse; however, probably due to dipole-dipole magnetic attraction, the average particle size diameter is close to 454 nm. The dark areas can be attributed to the crystalline Fe_3O_4 core, while the bright or clear zones are associated with the GMA-DETA coating.

The magnetic properties of the materials were determined using VSM (vibrating sample magnetometry). Figure SM2 (see Supplementary Material Section) shows their typical magnetization loops. There was no remanence and coercivity, contrary to certain supported-magnetite materials [10,11]. This means that MGMA-DETA sorbent is superparamagnetic. The saturation magnetization of MGMA and MGMA-DETA were found to be about 25.3 and 23.47 emu g^{-1} , respectively. These values are much smaller than the levels obtained for bulk phase magnetite (i.e., 49.21 emu g^{-1}).

XRD analysis was used for characterizing the crystalline structure of the material, which is induced by the magnetite core (Figure SM3, see Supplementary Material Section). The XRD pattern shows a limited number of peaks characteristics of iron oxides may be identified. The large fraction of polymer may contribute to explain the poor resolution of the XRD pattern. The peaks characteristics of magnetite (Fe_3O_4 [20,21]) are usually identified at indices: 30.2 (220), 35.6 (311), 43.3 (400), 53.7 (422), 57.7 (511) and 62.9 (440).

The thermogravimetric analysis (TGA) results showed that (Figure SM4, see Supplementary Material Section) the principle organic chains of MGMA-DETA began to degrade at about 240 °C and the final temperature of decomposition was approximately 440 °C. The average mass content of Fe_3O_4 on MGMA-DETA was confirmed to be about 23%.

3.2 Adsorption analysis

3.2.1 Effect of pH on the uptake

The pH value of the dye solution is an important factor for determination of the dye adsorption. This effect can be associated to sorbat speciation, to chemical properties of the sorbent (protonation/deprotonation of amino groups). The effect of the pH on the adsorption capacity of AY99 sorption by the MGMA-DETA sorbent was studied over the pH range from (1 to 9). The effect of the solution pH on AY99 elimination using the MGMA-DETA sorbent is shown in Figure 3a. The results suggested that the sorption capacity of AY99 on MGMA-DETA beads was pH-dependent and that maximum AY99 removal was obtained under acidic conditions (at pH 3-5). This could be due to the electrostatic interactions between anionic groups in AY99 and cationic protonated amino groups in the MGMA-DETA. The sulfonate groups

(SO₃Na) of AY99 could be converted in water to active negative sulfonate groups (SO₃⁻). Coupled with the protonation of amine groups in the adsorbents at low pH solutions, increases in the adsorption of AY99 molecules on the modified adsorbents [22]. However, increasing the acidity of the dye solution led to a slight decrease in AY99 removal. This could be due to the decrease in dye dissociation which leads to a lower concentration of the anionic dye species available to interact with the adsorbent's active sites. At pH higher than 5, the adsorption capacity of AY99 decreased, this may be the lower protonation extent of the amine groups on modified adsorbents. The minor change in sorption equilibrium at varied pH values may be attributed to the high pKa (10.45) of diethylenetriamine, the higher the pKa value of the ligand (DETA) grafted onto MCGMA sorbents, the wider is the effective pH range for anionic dye sorption [23].

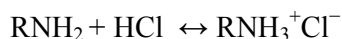
The mechanism of interaction of AY99 anions with the MGMA-DETA in acidic medium can be represented as follows:

The reactive dye molecule AY99-SO₃Na (The chemical structure of AY99 is shown in Scheme 1) dissociate as follows:

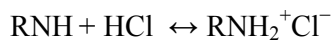


The amine groups of the MGMA-DETA are protonated under acidic conditions according to the following reaction:

For primary amino groups of MGMA-DETA



and for secondary amino groups of MGMA-DETA



The adsorption process proceeds through electrostatic interaction between the two counter ions ($\text{RNH}_3^+/\text{RNH}_2^+$ and AY99-SO_3^-).



Figure 3b shows the plot of equilibrium pH versus initial pH. It was observed in the plot that the final pH (pH_f) tended to change from its original pH (pH_i). The adsorption at $\text{pH}_i < 7.0$ resulted in pH_f changing to become less acidic, which might be due to the adsorption of H^+ ions alongside AY99 onto the sorbent surfaces. In contrast, the sorption at higher pH ($\text{pH}_i > 7$) resulted in pH_f being less basic, as a result of the increasing H^+ concentration. At higher pH values, the AY99 ion might be hydrolyzed and thus the proton (H^+) released into the medium solution, which would reduce the basicity of the equilibrium solution, along with AY99 usually dominates in the basic form of $\text{AY99-SO}_3\text{Na}$, removal of this basic form of dye reduces the basicity of the medium.

The MGMA-DETA sorbent maintained a significant sorption capacity at alkaline pH, which may be referred the feasibility of industrial application of the sorbent in the removal of AY99 from alkaline industrial effluent (effluent from textile industry usually at alkaline pH).

Iron concentration was analyzed during the adsorption of AY99 as a function pH. The concentration of the released iron was 4.1, 1.3, 0.12 and 0.0 at pH 0.5, 1.0, 2.0, 3.0, respectively. The reported values for the release of iron from magnetite at low pH: when the pH increases this release decreases until zero at pH 3. These values are consistent with the levels cited in our previous work [7]. The stability of the

composite adsorbent is an important issue to take into account and it sounds preferable managing the hybrid sorbent in solution whose pH is higher than pH 0.5–3.

3.2.2 Adsorption kinetics

The uptake kinetics of AY99 using the MGMA-DETA sorbent is shown in Figure 4. The kinetic profile is characterized by two phases in the uptake: (a) a first initial step that lasts for about 20 min and counts for more than 84.3 % of total adsorption, (a) a second step that takes about 90 min and corresponds to a much slower dye accumulation. The initial section of the curve corresponds to a great availability of reactive groups (surface coverage is progressively increasing) and a large concentration gradient between the solution and both the surface and the internal sorption sites. These two conditions may explain the fast initial accumulation of AY99 dye. The sorption mainly occurs on the reactive amino groups covering the surface of the sorbent. The second step, much slower, is controlled by the decrease of the concentration gradient and by the resistance to intraparticle diffusion and requires much longer time for reaching the equilibrium (i.e., about 90 min).

Actually the binding kinetics is controlled by a series of mechanisms including: (a) the bulk diffusion, (b) the resistance to film diffusion (or external diffusion), (c) the resistance to intraparticle diffusion, and (d) the proper reaction rate (chemical reaction rate) [24]. Usually a sufficient agitation allows neglecting the resistance to bulk diffusion and minimizes the resistance to film diffusion whose contribution in the control of uptake kinetics is mainly significant within the first minutes of contact. Experimental data have been modeled using simplified conventional equations to fit kinetic profiles and make possible the comparison of kinetic parameters for the two sorbents. Hence, the kinetics of AY99 sorption on the MGMA-DETA sorbent was

analyzed using the pseudo-first order rate equation (PFORE) [25], the pseudo-second order rate equation (PSORE) [26], the simplified resistance to intraparticle diffusion equation [27] and the Elovich equation [28]. These models and their linear forms are reported in Table SM1 (see Supplementary Material Section), where K_1 is the pseudo-first order rate constant (min^{-1}) of adsorption and q_e and $q(t)$ (mmol dye g^{-1}) are the amounts of AY99 sorbed at equilibrium and time t , respectively, k_2 is the pseudo-second order rate constant ($\text{g mmol}^{-1} \text{min}^{-1}$), K_i is the intraparticle diffusion rate ($\text{mmol g}^{-1} \text{min}^{-0.5}$), α the initial adsorption rate ($\text{mmol g}^{-1} \text{min}^{-1}$) and β the desorption constant (g mmol^{-1}). The validity of each model is checked by the correlation coefficient associated to the linear fits and χ^2 analysis was used to evaluate the best models to describe the metal ion sorption data. χ^2 was determined according to Eq. (4).

$$\chi^2 = \frac{(Q_{\text{exp}} - Q_{\text{cal}})^2}{Q_{\text{cal}}} \quad (4)$$

where Q_{exp} and Q_{cal} represent the experimental Q and calculated Q from the models, respectively. The best models for describing the kinetic data can be selected if R^2 is equal to or near 1 and χ^2 is as small as possible. Table 1 reports the parameters of the different models for the studied adsorbents. Systematically, the best correlation coefficients were found for the PSORE model; this is confirmed by the plot of experimental data according the linearized forms of these models: Figure SM 5a and Figure SM5b (see Supplementary Material Section) for PFORE and PSORE, respectively, show a best fit of kinetic profiles by PSORE. In addition, the comparison of equilibrium adsorption capacities for the calculated values and the experimental values are only consistent for the PSORE model: the equilibrium sorption capacities are found close to $0.242 \text{ mmol dye g}^{-1}$. PSORE modeling gave value of 0.246 mmol

dye g^{-1} closer from experimental values than PFORE (0.057 mmol dye g). It was more likely to reflect that the rate-determining step might be chemical sorption and that the sorption behavior might involve an ion exchange mechanism.

However, the PSORE describes kinetics data through a global approach, and does not take into account the contribution of diffusion mechanisms in the control of the kinetics. Under these conditions, the kinetic parameters should be considered as apparent rate coefficients. The influence of resistance to intraparticle diffusion has been approached using a simplified model: the so-called Weber et Morris plot (See Table 1). The intraparticle diffusion model provides a more comprehensive approach for defining of adsorption mechanism, and the plot generally allows identifying different successive steps in the global process [27]. The Weber and Morris shows multi-linear sections (Figure. SM6a, see Supplementary Material Section), i.e., three linear sections (on the plot $q(t)$ vs. $t^{0.5}$) with fast kinetics in first step followed by the gradual attainment of equilibrium, and a pseudo saturation plateau. The multi-linear plot does not pass through the origin suggesting that the resistance to intraparticle diffusion is not the sole rate-limiting step: other steps, e.g. resistance to film diffusion and/or reaction rate, are probably involved in the control of uptake kinetics (Table 1, Figure SM6a). We can assume that the first linear section corresponds to a regime controlled by the resistance to film diffusion and that the binding is limited in this stage at the adsorption of external adsorption sites or on the macropores in the first external layers of the material. The second section is characterized by a much lower kinetic rate and leads to a slow approach to equilibrium with the control by the resistance to intraparticle diffusion (into internal macroporous and mesoporous network). The last step is very slow and represents only a few percentage of the total adsorption: this phase can be associated to the resistance to diffusion in the

microporous network of the adsorbent. In addition the progressive saturation of available and accessible adsorption sites influences the local equilibrium on the surface between surface sorption and desorption. The low values of intraparticle rate constants (K_i) appearing in Table 1 with values available in the literature indicates that the adsorbents are significantly affected by the resistance to intraparticle diffusion.

The Elovich equation was developed for modeling chemisorption processes [28]. Table 1 displays the model equation and its linearization as well the plots to be used for determining the parameters. The values of α and β were determined from the intercept and slope, respectively, of the linear plot of q_t vs $\ln t$ (Figure SM6b, see Supplementary Material Section). The values of α for the sorption of AY99 dye on the modified sorbents is $1.47 \text{ (mmol g}^{-1} \text{ min}^{-1})$. This value reflects the high affinity and fast kinetics of AY99 onto the MGMA-DETA sorbent, which may be attributed to the high concentration of active sites on the sorbent surface allowed for reacting with AY99 anions. The values of β (desorption constant) is found to be $33.09 \text{ g mmol}^{-1}$. This value is compatible with the levels cited in our previous work [29]. This is another confirmation of the high affinity of the resin for AY99 anions.

3.2.3 Adsorption isotherms

The adsorption isotherms reveal the specific relation between the concentration of adsorbate and the adsorption capacity of an adsorbent at a constant temperature [7]. Adsorption isotherms provide some information on how an adsorption system proceeds, and indicate how molecules of adsorbate interact with adsorbent [7]. The Langmuir [30], Freundlich [31], Dubinin–Radushkevich (DR) [32], and Temkin [33] isotherm models were used to explain the sorption of AY99 on the MGMA-DETA

sorbent. The linear and nonlinear forms of the isotherm models are shown in Table SM2 (see Supplementary Material Section), and their parameters are shown in Table 2. where q_e the adsorbed amount of dye at equilibrium concentration (mmol g^{-1}), $q_{m,L}$ is the maximum sorption capacity (corresponding to the saturation of the monolayer, mmol g^{-1}) and K_L is the Langmuir binding constant which is related to the energy of sorption (L mmol^{-1}), C_e is the equilibrium concentration of AY99 dye in solution (M). K_F (mmol g^{-1}) (L mmol^{-1}) $^{1/n}$ and n are the Freundlich constants related to the sorption capacity and intensity, respectively. K_{DR} ($\text{J}^2 \text{mol}^{-2}$) is a constant related to the sorption energy, q_{DR} (mmol g^{-1}) is the theoretical saturation capacity, ϵ ($\text{J}^2 \text{mol}^{-2}$) is the Polanyi potential. R ($8.314 \text{ J mol}^{-1}\text{K}^{-1}$) is the gas constant, T is the temperature where the adsorption occurs, A_T (L mg^{-1}) is the Temkin isotherm constant, b_T (J mol^{-1}) is Temkin constant in relation to heat of adsorption.

The Langmuir isotherm models were found to be the most suitable models for describing the isotherm for the adsorption of the AY99 dye into the MGMA-DETA sorbent. However, from the isotherm fitting in (Figure SM7a, see Supplementary Material Section), the Freundlich lines deviated from the experimental data points. The isotherm fitting was plotted on the basis of the nonlinear equations using the model constant parameters obtained from the linear equation plot analysis. Via comparison of the R^2 values, the Langmuir isotherm resulted in very good fitting, with R^2 value of > 0.997 . In addition, the Q_m calculated from the Langmuir isotherm was close to the experimental Q_{max} . The isotherm model fittings as shown in Figure 5 also show that the theoretical Langmuir lines were closer to the experimental data. The adsorption process is schematically shown in Scheme 2. Analysis of isotherm parameters proposed by Dubinin and Radushkevich (Table 2). This isotherm was developed taking into account the effect of the porous structure of the sorbent, and the

energy involved in the sorption process. The Polanyi potential (ε) given as Eq. (5) [32]:

$$\varepsilon = RT \ln \left(1 + \frac{1}{C_{\text{eq}}} \right) \quad (5)$$

R is the universal gas constant ($8.314 \text{ J mol}^{-1} \text{ K}^{-1}$) and T is the absolute temperature (K). The slope of the plot of $\ln q_{\text{eq}}$ vs. ε^2 (Figure SM8a, see Supplementary Material Section) gives K_{DR} and the intercept yields Q_{DR} (Table 2). The D–R constant (K_{DR}) can give valuable information regarding the mean energy of sorption (E_a , J mol^{-1}) by Eq. (6):

$$E_a = \frac{1}{(2K_{\text{DR}})^{0.5}} \quad (6)$$

The results of D–R isotherm are reported in Table 2. The value of the mean energy of sorption is $17.677 \text{ kJ mol}^{-1}$: this is consistent with the proposed mechanism of chemisorption. Indeed, it is generally admitted that 8 kJ mol^{-1} is the limit energy for distinguishing physical (below 8 kJ mol^{-1}) and chemical sorption. A comparison of the correlation coefficient values obtained from the Langmuir, Freundlich and D–R isotherm models in Table 2 reveals that the correlation coefficients for the Langmuir isotherm are somewhat higher than those for the Freundlich, D–R isotherm and Temkin models. This result suggests that the binding of dye ions may occur as a monolayer on the surface of the sorbent and that the uptake occurs on a homogenous surface by monolayer sorption. This should be confirmed by experimental observation for confirmation. The uptake can be described in terms of chemisorption as ion exchange mechanism (Protonated amino groups of DETA moiety may be exchanged with anionic dye, depending on the pH). The presence the same type of functional

groups is comforting the hypothesis of homogeneous surface (or homogeneous energies of sorption). The ranking of the models as follow: Langmuir > Temkin > Dubinin and Radushkevich > Freundlich.

3.2.4 Influence of temperature

It is important to investigate the effect of temperature on adsorption in a view of practical application. The adsorption experiments were carried out at five different temperatures including 20, 25, 30, 35 and 45°C. The adsorption capacity slightly increases from 0.240 to 0.247 mmol g⁻¹ with the increase in the temperature from 20 to 45°C. This behavior confirms that the adsorption process of AY99 onto MGMA-DETA is endothermic. This observation can be attributed to increasing of the mobility of the dye molecules and rate of diffusion of adsorbate molecules across the surface of adsorbent with increasing temperature, which leads to an increase in the adsorption capacity [34]. The adsorption equilibrium constant, K_c was determined (Eq. 7) and used with the van't Hoff equation (Eq. 10) and conventional thermodynamic equation (Eq. 9) for evaluating the thermodynamic constants of the sorbents (i.e., the standard enthalpy change, ΔH° , the standard free Gibbs energy, ΔG° , and the standard entropy change, ΔS°).

$$K_c = \frac{q_e}{C_e} \quad (7)$$

where q_e and C_e are equilibrium concentrations of AY99 on the adsorbent and in the solution, respectively.

$$\Delta G^\circ = -RT \ln K_c \quad (8)$$

$$\Delta G^\circ = \Delta H^\circ - T\Delta S^\circ \quad (9)$$

Therefore the van't Hoff equation becomes:

$$\ln K_c = \frac{-\Delta H^\circ}{RT} + \frac{\Delta S^\circ}{R} \quad (10)$$

The value of standard enthalpy change (ΔH°) and standard entropy change (ΔS°) for the adsorption process are thus determined from the slope and intercept of the plot of $\ln K_c$ versus $1/T$ (Figure 6): the values of thermodynamic parameters are reported in Table 3. The positive value of ΔH° confirms the endothermic nature of adsorption process. The negative values of ΔG° indicate that the adsorption reaction is spontaneous. The increase in the negativity of ΔG° with increasing temperature confirms that the “favorability” increases with temperature. On the other hand, the positive value of the entropy change (ΔS°) mean that the “disorder” of the system increases after dye adsorption.

In industries and water purification plants the optimum temperature at which the adsorption is highly feasible and spontaneous is essential. The adsorption of dyes onto adsorbent surfaces may be either spontaneous or non-spontaneous in function of temperature. The limit temperature value corresponding to a null value of standard free energy can thus be deduced from Eq. 11. The range of temperature can be predicted from the value of temperature at which the standard free energy is zero (T_0), and then the minimal temperature for the process to being spontaneous.

$$T_0 = \frac{\Delta H^\circ}{\Delta S^\circ} \quad (11)$$

Here, the calculated value of zero standard free energy temperature (T_0) is 246.3 K. The low T_0 values indicate the feasibility of AY99 removal at very low temperature by the studied adsorbents.

3.2.5 Effect of adsorbent dosage

The adsorption of AY99 on the MGMA-DETA sorbent was studied by changing the quantity of adsorbent range of (0.01 to 0.1) g 25 mL⁻¹, with the dye concentration of 5x10⁻⁴M at ± 1 °C and pH of 3.0. The results in Figure 7a show the AY99 adsorption capacity as a function of adsorbent amount. It has been found that the adsorption capacity decreases from 0.293 to 0.124 mmol/g when the dose of MGMA-DETA increases from 0.01 to 0.1 g 25 mL⁻¹. Figure 7b shows the effect of dose on the equilibrium concentration (C/C₀) of AY99 by the MGMA-DETA sorbent. As the dose increases, the equilibrium concentration of AY99 is decreased, which is due to the increase in the adsorbent surface area of the adsorbent. The results shown indicate that the removal efficiency increases up to 99.74% (C/C₀= 0.0025) at adsorbent dose of 0.1g 25 mL⁻¹. The surface of the adsorbent is composed of active sites with a spectrum of binding energies [7]. At the low dose of adsorbent, all of the sites are exposed entirely and the adsorption on the surface is saturated faster showing a higher adsorption capacity. An increase in the mass of adsorbent leads to a decrease in equilibrium adsorption capacity per unit weight of the adsorbent (q_e) because there are excess adsorbent for the limited amount of AY99 ions in the solution. According to the result, the dose of 0.01g 25 mL⁻¹ will achieve the maximum loading capacity for the sorbent, and the dose of 0.1 g 25 mL⁻¹ will achieve the maximum removal efficiency 99.74% (C/C₀= 0.0025). So the determination of the optimum adsorbent dose depends on the design and purpose of treatment process. Thus if the water quality standard set by WHO is the target, a larger amount of adsorbent is better (0.1 g 25 mL⁻¹), and if the maximum loading of the sorbent per unit mass is the target, the dose of 0.01 g 25 mL⁻¹ is more suitable.

3.2.6. Effect of ionic strength (addition of NaCl)

The effect of chloride ions on AY99 removal was examined, by addition of increasing concentrations of NaCl (Figure 8). For the studied adsorbents increasing the amount of NaCl slightly decreases the sorption capacity: the sorption capacity decreases by 20%, when NaCl concentration reaches 20 g L^{-1} . This is probably due to the competitor effect of chloride anions against AY99 anions for interaction with adsorption sites. It is noteworthy, that when even NaCl concentration reaches 40 g L^{-1} the reduction in the adsorption capacity decreases by 1.5%, this indicates that even under these drastic conditions a high adsorption capacity is maintained.

3.3. Adsorbent regeneration

Regeneration of the MGMA-DETA was performed by using 1.0 M NaOH. After regeneration, the sorbent was again carefully washed with distilled water to become ready for the second run of uptake. The regeneration efficiency for each adsorption/desorption cycle was found to be 88.2, 86.1, 84.5%. This indicates that sorbent has good performance for repeated use up to at least 4 cycles.

3.4. Comparison of adsorption of AY99 dye with various sorbents

Table 4 shows the comparison of maximum sorption capacities of the MGMA-DETA with a series of values found in the literature (together with the best operating conditions reported by respective authors). A direct comparison of sorption performance is difficult due to different experimental conditions; however, this is a useful criterion for roughly evaluating the potential of these materials. The MGMA-DETA adsorbent has a adsorption capacity of the same order of magnitude as other sorbents; although Cotton cellulose based cationic adsorbent [35], Stipa Tenacissima

L Cationized Fibers [37], Cationized Sawdust [39] and Polyacrylonitrile/activated carbon composite [40] showed better adsorption capacity. When taking into account only the organic compartment in the MGMA-DETA that represents about 77 % of total sorbent mass, the sorption capacity of MGMA-DETA increases to 0.298.

The other advantage of MGMA-DETA sorbent is associated to the enhancement of recovery facilities (solid/liquid separation) related to the paramagnetic properties of the composites (magnetic core) that can be beneficial for the management and operating of dye sorption in hazardous environment. It is noteworthy that the MGMA-DETA sorbent has an important advantage related to their fast kinetics. The high sorption capacity of the MGMA-DETA adsorbents towards AY99 dye reveals that adsorbent could be promising for practical application in AY99 dye removal from wastewater.

4. Conclusion

The functionalization of magnetic glycidylmethacrylate (crosslinked with N,N'-methylenebisacrylamide) with grafting of diethylenetriamine allows manufacturing a very efficient adsorbent. The prepared adsorbent was characterized via FTIR, SEM, XRD and TGA. This adsorbent exhibited high adsorption capacity towards AY99. The maximum monolayer adsorption capacities are $0.242 \text{ mmol g}^{-1}$ at pH 3 and 25 °C. The nature of interaction between the dye anions and the adsorbent was found to be dependent upon the acidity of the medium. The adsorption process carries out by anion exchange mechanism; however the adsorbent maintained a significant adsorption capacity at alkaline pH. The adsorption isotherms are well fitted by the Langmuir equation. Uptake kinetics is correctly fitted by the pseudo-second order rate equation. The thermodynamic parameters have been determined: the reaction is

endothermic, spontaneous. The randomness of the system increases with AY99 adsorption. Even under drastic conditions of high ionic strength, the sorbent maintained its high sorption capacity. The adsorbents can be used successfully up to 4 times without significant loss of its original efficiency regenerated by 1.0 M NaOH. This means that the studied sorbent is a promising sorbent for the efficient removal of AY99 dye from wastewater of textile industry.

References

- [1] R.A. Rudel, K.R. Attfield, J.N. Schifano, J.G. Brody, Animals signal new directions for epidemiology, chemicals testing, and risk assessment for breast cancer prevention, *Cancer* 109 (2007) 2635-2666.
- [2] N. Mathur, P. Bhatnagar, P. Nagar, M.K. Bijarnia, Mutagenicity assessment of effluents from textile/dye industries of Sanganer, Jaipur (India): a case study, *Ecotoxicol. Environ. Safe.* 61 (2005) 105–113.
- [3] L.F. Barrios-Ziolo, L.F. Gaviria-Restrepo, E.A. Agudelo, S.A. Cardona-Gallo, Technologies for the removal of dyes and pigments present in wastewater. A review, *DYNA-Colombia* 82 (2015) 118–126.
- [4] K.Z. ELwakeel, Removal of reactive black 5 from aqueous solutions using magnetic chitosan resins, *J. Hazard. Mater.* 167 (2009)383–392.
- [5] N.M. Mahmoodi, Surface modification of magnetic nanoparticle and dye removal from ternary systems, *J. Ind. Eng. Chem.* 27 (2015) 251–259.
- [6] R.F. Gomes, A.C. Neto de Azevedo, A.G.B. Pereira, E.C. Muniz, A.R. Fajardo, F.H.A. Rodrigues, Fast dye removal from water by starch-based nanocomposites, *J. Colloid Interface Sci.* 454 (2015) 200–209.

- [7] K.Z. Elwakeel, E. Guibal, Selective removal of Hg(II) from aqueous solution by functionalized magnetic-macromolecular hybrid material, *Chem. Eng. J.* 281 (2015) 345–359.
- [8] A. Islam, N. Zaidi, H. Ahmad, S. Kumar, Amine-functionalized mesoporous polymer as potential sorbent for nickel preconcentration from electroplating wastewater, *Environ. Sci. Pollut. Res.* 22 (2015) 7716–7725.
- [9] Z. Zhang, F. Wang, W. Yang, Z. Yang, A. Li, A comparative study on the adsorption of 8-amino-1-naphthol-3,6- disulfonic acid by a macroporous amination resin, *Chem. Eng. J.* 283 (2016) 1522–1533.
- [10] A.A. Galhoum, M.G. Mahfouz, A.A. Atia, S.T. Abdel-Rehem, N.A. Gomaa, T. Vincent, E. Guibal, Amino acid functionalized chitosan magnetic nano-based particles for uranyl sorption, *Ind. Eng. Chem. Res.* (2015) DOI: 10.1021/acs.iecr.5b03331
- [11] A. A. Galhoum . M.G. Mahfouz.S.T. Abdel-Rehem. N.A. Gomaa.A.A. Atia. T. Vincent, E. Guibal, Diethylenetriamine-functionalized chitosan magnetic nanobased particles for the sorption of rare earth metal ions [Nd(III), Dy(III) and Yb(III)], *Cellulose* 22 (2015) 2589–2605.
- [12] O.A. Abdel Moamen, H.A. Ibrahim, N. Abdelmonem, I.M. Ismail, Thermodynamic analysis for the sorptive removal of cesium and strontium ions onto synthesized magnetic nano zeolite, *Microporous Mesoporous Mater.* 223 (2016) 187–195.
- [13] D. Yuan, L. Chen, X. Xiong, L. Yuan, S. Liao, Y. Wang, Removal of uranium (VI) from aqueous solution by amidoxime functionalized superparamagnetic

- polymer microspheres prepared by a controlled radical polymerization in the presence of DPE, *Chem. Eng. J.* 285 (2016) 358–367.
- [14] A.M. Donia, A.A. Atia, K.Z. Elwakeel. Recovery of gold(III) and silver(I) on a chemically modified chitosan with magnetic properties, *hydrometallurgy* 87 (2007) 197–206.
- [15] S. Bao, L. Tang, K. Li, P. Ning, J. Peng, H. Guo, T. Zhu, Y. Liu, Highly selective removal of Zn(II) ion from hot-dip galvanizing pickling waste with amino-functionalized Fe₃O₄@SiO₂ magnetic nano-adsorbent, *J. Colloid Interface Sci.* 462 (2016) 235–242.
- [16] N. Khoddami, F. Shemirani, A new magnetic ion-imprinted polymer as a highly selective sorbent for determination of cobalt in biological and environmental samples, *Talanta* 146 (2016) 244–252.
- [17] A.A. Atia, A.M. Donia, K.Z. ELwakeel, Selective separation of Mercury(II) using magnetic chitosan resin modified with Schiff's base derived from thiourea and glutaraldehyde, *J. Hazard. Mater.* 151 (2008) 372–379.
- [18] R. Massart, Preparation of aqueous magnetic liquids in alkaline and acidic media, *IEEE Trans. Magn.* 17 (1981) 1247-1249.
- [19] C. Liu, R. Bai, L. Hong, Diethylenetriamine-grafted poly(glycidyl methacrylate) adsorbent for effective copper ion adsorption, *J. Colloid Interface Sci.* 303 (2006) 99–108.
- [20] Y.-T. Zhou, H.-L. Nie, C. Branford-White, Z.-Y. He, L.-M. Zhu, Removal of Cu²⁺ from aqueous solution by chitosan-coated magnetic nanoparticles modified with α -ketoglutaric acid, *J. Colloid Interface Sci.* 330 (2009) 29-37.

- [21] G.-Y. Li, Y.-R. Jiang, K.-L. Huang, P. Ding, Preparation and properties of magnetic Fe₃O₄-chitosan nanoparticles, *J. Alloys Compd.* 466 (2008) 451-456.
- [22] K.Z. Elwakeel, M.A. Abd El-Ghaffar, S.M. El-kousy, H.G. El-shorbagy, Synthesis of new ammonium chitosan derivatives and their application for dye removal from aqueous media, *Chem. Eng. J.* 203 (2012) 458-468.
- [23] S. Chatterjee, T. Chatterjee, S.H. Woo, Influence of the polyethyleneimine grafting on the adsorption capacity of chitosan beads for Reactive Black 5 from aqueous solutions, *Chem. Eng. J.* 166 (2011) 168-175.
- [24] K.Z. Elwakeel, E. Guibal, Arsenic(V) sorption using chitosan/Cu(OH)₂ and chitosan/CuO composite sorbents, *Carbohydr. Polym.* 134 (2015) 190-204.
- [25] S. Lagergren, About the theory of so-called adsorption of soluble substances, *Kungliga Swenska Vet.* 24 (1898) 1-39.
- [26] Y.S. Ho, G. McKay, Pseudo-second order model for sorption processes, *Process Biochem.* 34 (1999) 451-465.
- [27] W.J. Weber, J.C. Morris, Kinetics of adsorption on carbon from solutions, *J. Sanitary Eng. Div. ASCE* 89 (1963) 31-60.
- [28] J. Zeldowitsch, The catalytic oxidation of carbon monoxide on manganese dioxide, *Acta Physicochim. URSS* 1 (1934) 364-449.
- [29] K.Z. Elwakeel, M.M. Alrekaby, Efficient removal of reactive black 5 from aqueous media using glycidyl methacrylate resin modified with tetraethelenepentamine, *J. Hazard. Mater.* 188 (2011) 10-18.

- [30] I. Langmuir, The adsorption of gases on plane surfaces of glass, mica and platinum, *J. Amer. Chem. Soc.* 40 (1918) 1361-1402.
- [31] H.M.F. Freundlich, Uber die adsorption in lasungen, *Z. Phys. Chem.* 57 (1906) 385-470.
- [32] M.M. Dubinin, E.D. Zaverina, L.V. Radushkevich, Sorption and structure of active carbons.I. Adsorption of organic vapors, *Zh. Fiz. Khim.* 21 (1947) 1351-1362.
- [33] M.I. Temkin, V. Pyzhev, Kinetics of ammonia synthesis on promoted iron catalysts. *Acta physiochim. URSS* 12 (1940) 217–222.
- [34] A.S. Patra, S. Ghorai, S. Ghosh, B. Mandal, S. Pal, Selective removal of toxic anionic dyes using a novel nanocomposite derived from cationically modified guar gum and silica nanoparticles, *J. Hazard. Mater.* 301 (2016) 127–136.
- [35] V. Kumar, N.K. Goel, Y.K. Bhardwaj, S. Sabharwal, L. Varshney, Development of functional adsorbent from textile cotton waste by radiation induced grafting process: equilibrium and kinetic studies of acid dye adsorption, *Sep. Sci. Technol.* 47 (2012) 1937–1947.
- [36] M.M.R. Khan, M. Ray, A.K. Guha, Mechanistic studies on the binding of Acid Yellow 99 on coir pith, *Bioresour. Technol.* 102 (2011) 2394–2399.
- [37] A. El Ghali, M.H.V. Baouab, M.S. Roudesli, Stipa Tenacissima L Cationized fibers as adsorbent of anionic dyes, *J. Appl. Polym. Sci.* 116 (2010) 3148–316.
- [38] M.H.V. Baouab, H. Zghida, R. Gauthier, H. Gauthier, Cationized nylon as adsorbent for anionic residual dyes, *J. Appl. Polym. Sci.* 91 (2004) 2513–2522.

- [39] M.H.V. Baouab, R. Gauthier, H. Gauthier, M.E.B. Rammah, Cationized sawdust as ion exchanger for anionic residual dyes, *J. Appl. Polym. Sci.* 82 (2001) 31–37.
- [40] A.A. El-Bindary, M.A. Hussien, M.A. Diab, A.M. Eessa, Adsorption of Acid Yellow 99 by polyacrylonitrile/activated carbon composite: Kinetics, thermodynamics and isotherm studies, *J. Mol. Liq.* 197 (2014) 236–242.

Tables

Table 1: Kinetic parameters for AY99 adsorption

PFORE				PSORE				Weber and Morris model			Elovich equation		
k_1	$q_{e, calc}$	R^2	χ^2	k_2	$q_{e, calc}$	R^2	χ^2	k_i	X	R^2	α	β	R^2
(a)	(b)			(c)	(b)			(d)			(e)	(f)	
0.046	0.057	0.948	0.60	1.651	0.246	0.999	0.00006	K_{i1}	0.015	0.133	0.979		
								K_{i2}	0.001	0.230	0.882	1.47	33.09
								K_{i3}	8.92E-05	0.241	0.857		0.936

Units: (a): min^{-1} ; (b): mg g^{-1} ; (c): $\text{g mg}^{-1} \text{min}^{-1}$; (d): $\text{mg g}^{-1} \text{min}^{0.5}$; (e): $\text{mg g}^{-1} \text{min}^{-1}$; (f): g mg^{-1} .

Table 2: Parameters of the sorption isotherm models

Langmuir model					Freundlich model			Dubinin-Radushkevich (D-R) model					Temkin model		
$q_{m, \text{exp}}$	$q_{m, L}$	K_L	R^2	χ^2	n	K_F	R^2	Q_{DR}	K_{DR}	Ea	R^2	χ^2	A_T	b_T	R^2
(a)	(a)	(b)				(c)		(a)	(d)	(kJ mol ⁻¹)			(e)	(f)	
0.379	0.385	330.21	0.997	0.00007	0.832	444.24	0.800	0.391	1.60E-09	17.677	0.836	0.0003	1.976	14.205	0.919

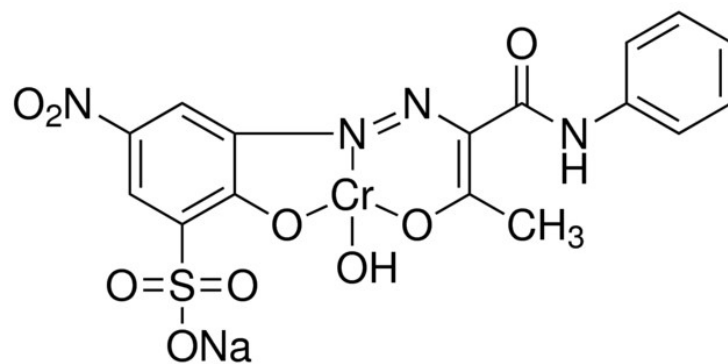
Units: (a): mmol g⁻¹; (b): L mmol⁻¹; (c): mmol g⁻¹ (L mmol⁻¹)^{1/n}; (d): J² mol⁻²; (e): kJ mol⁻¹; (f): L mol⁻¹.

Table 3: Standard enthalpy, entropy and free energy changes for AY99 adsorption

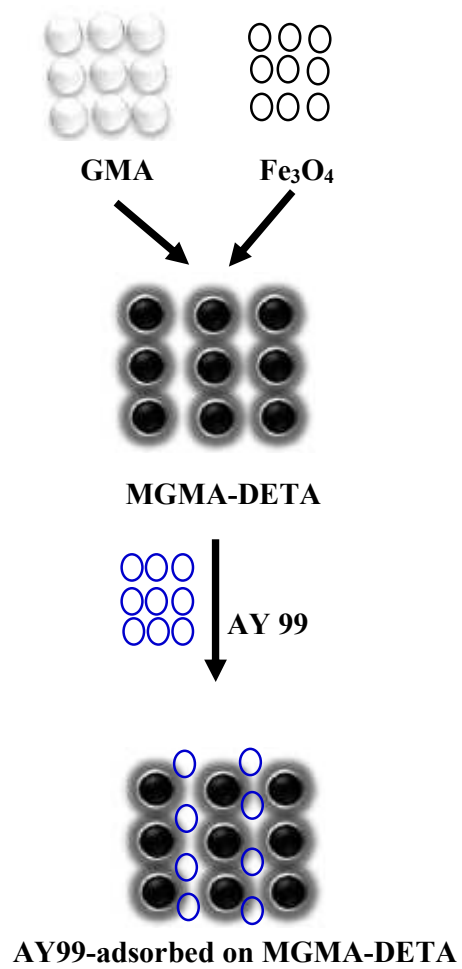
ΔH° (kJ mol ⁻¹)	ΔS° (J mol ⁻¹ K ⁻¹)	T_0 (K)	ΔG° (kJ mol ⁻¹)				
			293 K	298 K	303 K	308 K	318 K
43.45	176.41	246.32	-8.23	-9.11	-9.99	-10.88	-12.64

Table 4: Comparison of sorption performance for AY 99 dye with various adsorbents

Adsorbent material	Initial pH	Contact time (min)	Temperature (°C)	Initial concentration (mM)	Sorbent dosage (g L⁻¹)	Sorption capacity (mmol g⁻¹)	References
Cotton cellulose based cationic adsorbent	-	400	25	-	8.0	0.920	[34]
Coir pith	2.00	200	30	0.20	8.0	0.015	[35]
Stipa Tenacissima L Cationized Fibers	7.00	120	20	2.01	1.0	1.341	[36]
Cationized Nylon	6.5	180	20	-	10.0	0.195	[37]
Cationized Sawdust	-	120	20	-	10.0	0.543	[38]
Polyacrylonitrile/activated carbon composite	1.1	90	25	0.12	0.4	0.300	[39]
Diethylenetriamine functionalized magnetic Glycidyl methacrylate - N,N' methylenebisacrylamide	3	90	25	0.5	2.0	0.242	[This work]



Scheme 1: Chemical structure of Acid Yellow 99 dye



Scheme 2: Schematic diagram of AY99 adsorption on MGMA-DETA

List of Figures - Captions

Figure 1: Scanning electron micrographs of; (a) unloaded MGMA-DETA, (b) AY99-loaded MGMA-DETA.

Figure 2: Transmission photographs of the MGMA-DETA adsorbent

Figure 3: pH effect on AY99 adsorption using the MGMA-DETA adsorbent: (T: $25 \pm 1^\circ\text{C}$; C_0 : $5 \times 10^{-4}\text{M}$).

Figure 4: AY99 uptake kinetics using the MGMA-DETA adsorbent: (pH 3; T: $25 \pm 1^\circ\text{C}$; C_0 : $5 \times 10^{-4}\text{M}$).

Figure 5: AY99 adsorption isotherms onto the MGMA-DETA adsorbent (solid lines are stimulated from Langmuir equation) (pH 3; T: $25 \pm 1^\circ\text{C}$).

Figure 6: van't Hoff plots for AY99 adsorption onto the MGMA-DETA adsorbent.

Figure 7: Effect of sorbent dose (SD) on AY99 adsorption using MGMA-DETA: (a) sorption capacity vs. SD, (b) relative residual concentration (C/C_0) vs. SD (C_0 : $5 \times 10^{-4}\text{M}$; T: $25 \pm 1^\circ\text{C}$; pH 3).

Figure 8: Influence of NaCl on AY99 adsorption onto the MGMA-DETA adsorbent (C_0 : $5 \times 10^{-4}\text{M}$; initial pH 3; T: $25 \pm 1^\circ\text{C}$; sorbent dosage: $0.05\text{ g } 25\text{ mL}^{-1}$).

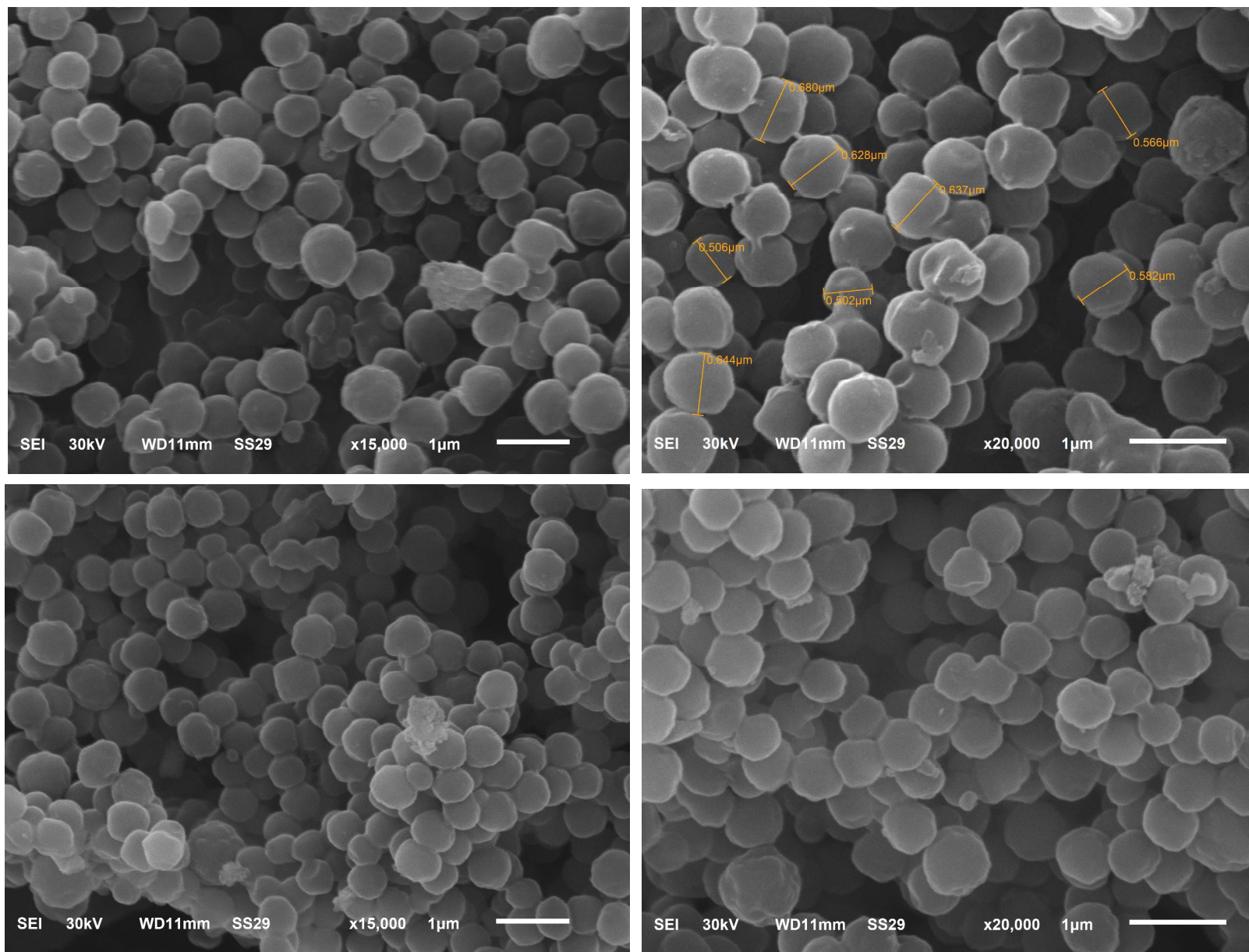
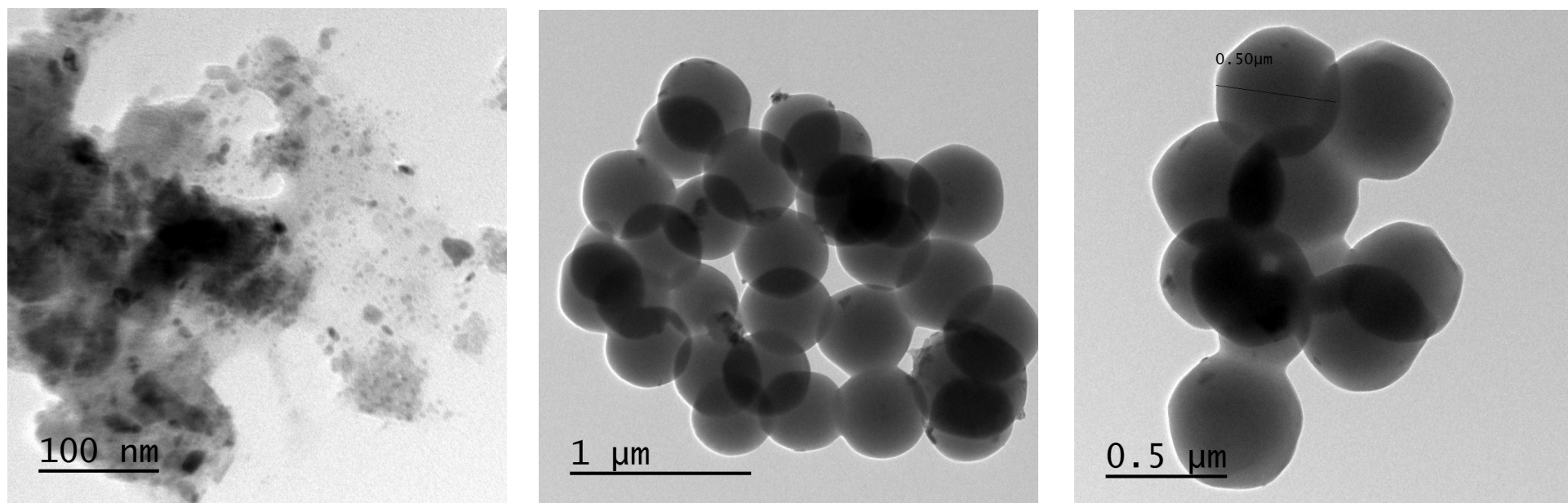
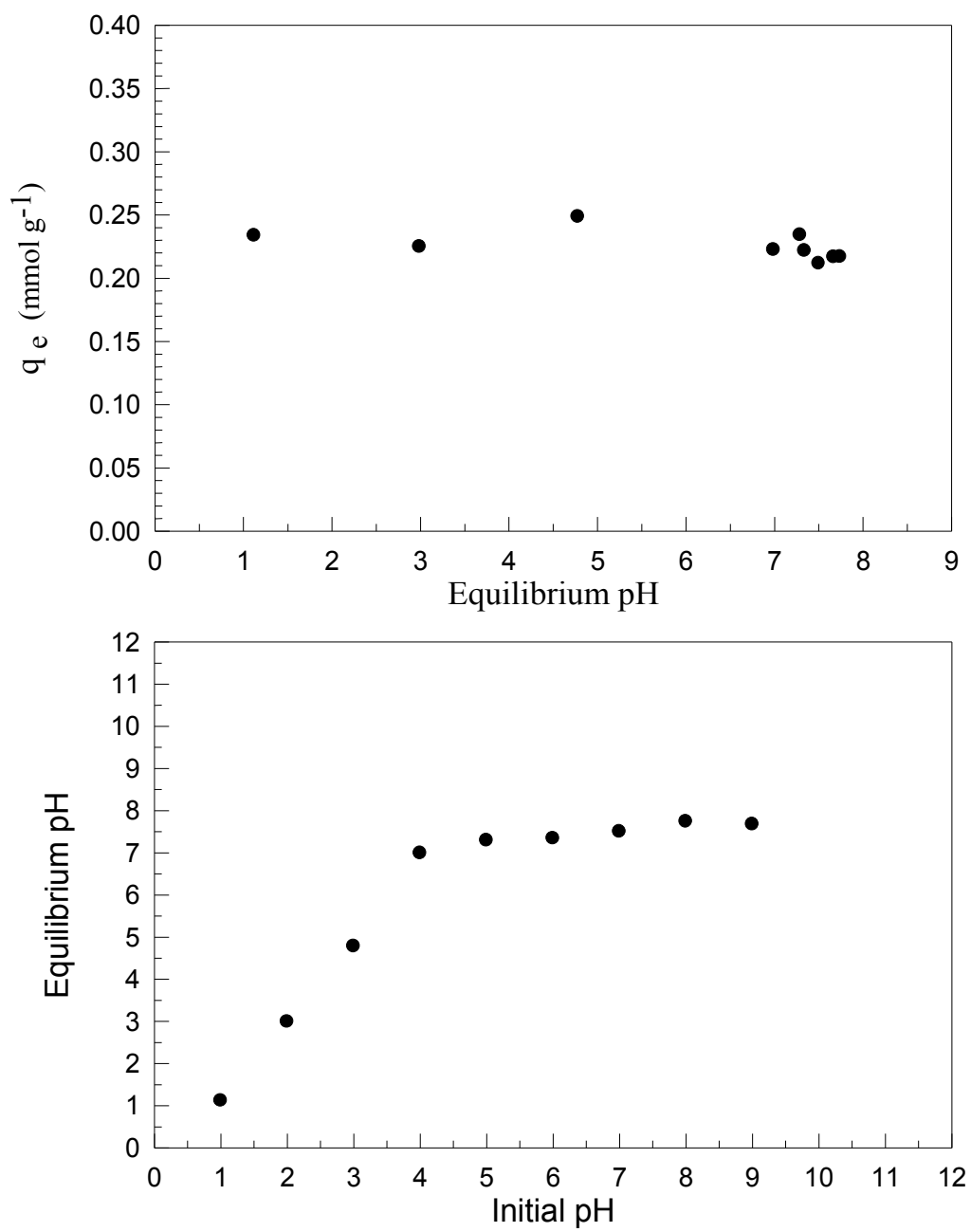
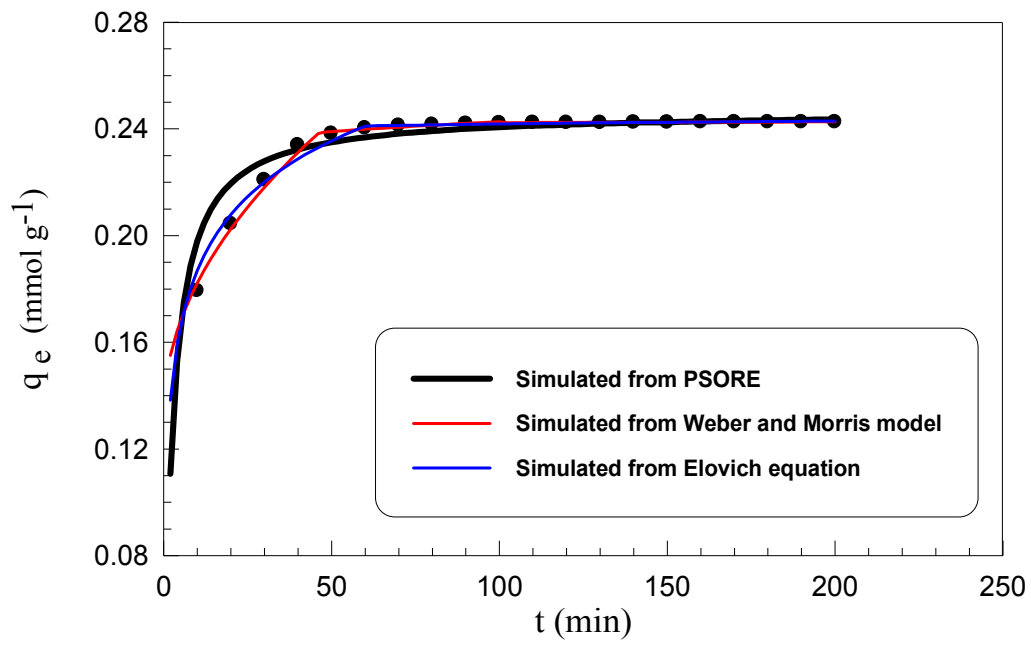
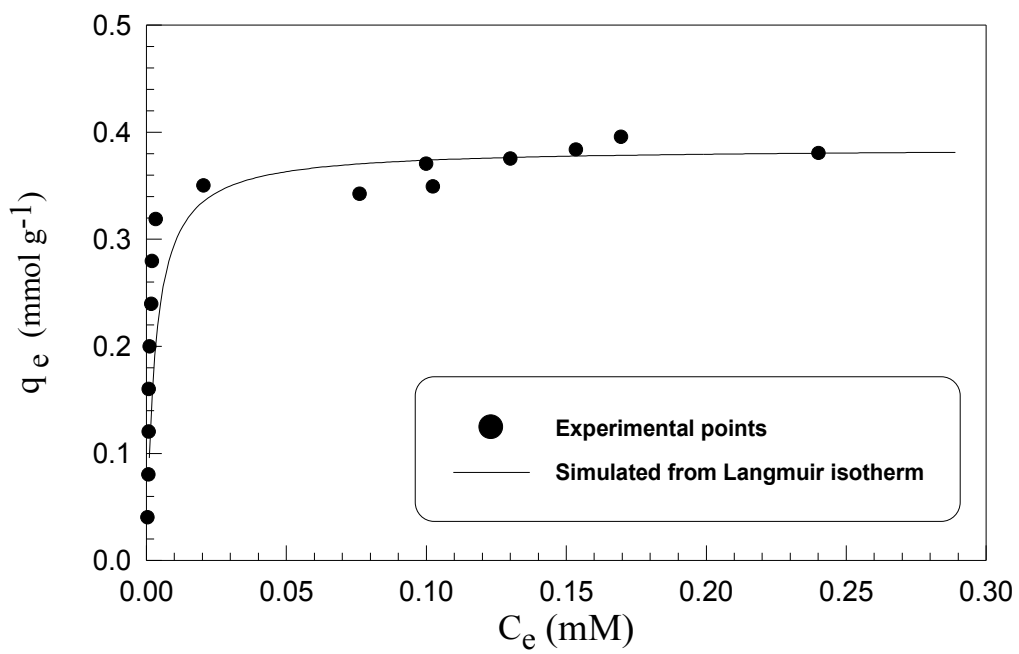


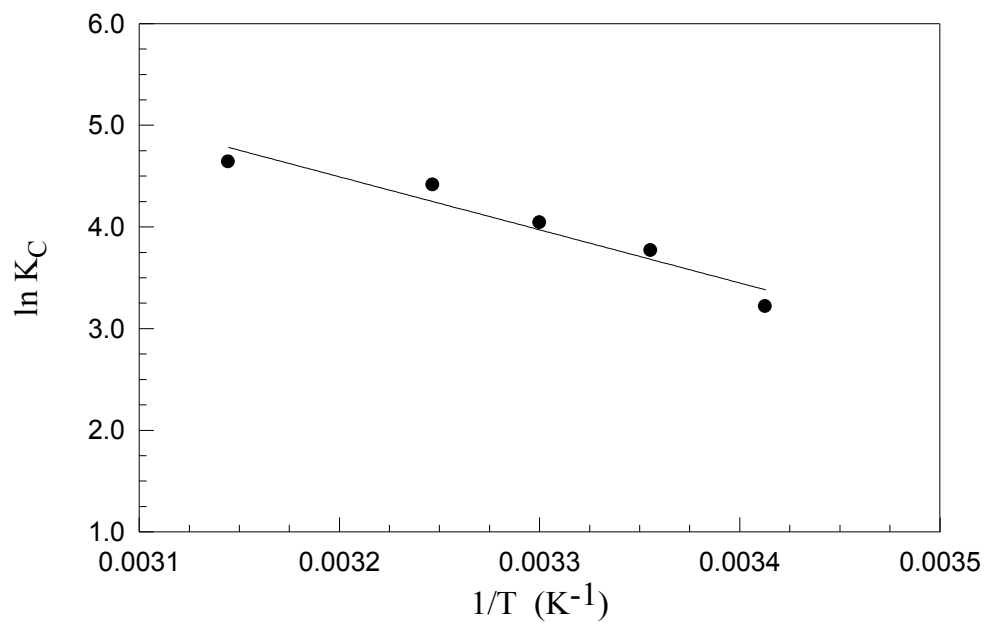
Fig. 1

**Fig. 2**

**Fig. 3**

**Fig.4**

**Fig. 5**

**Fig. 6**

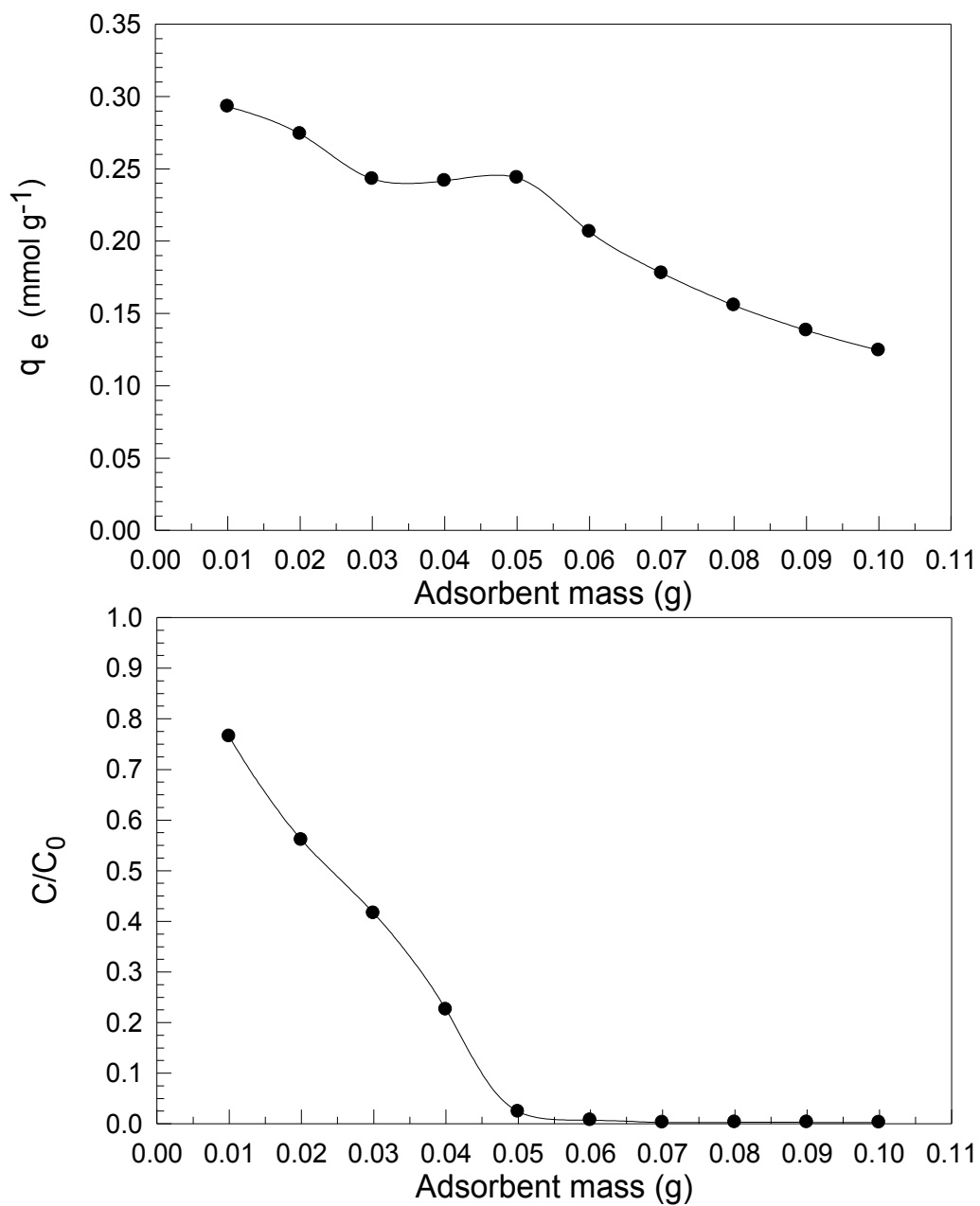
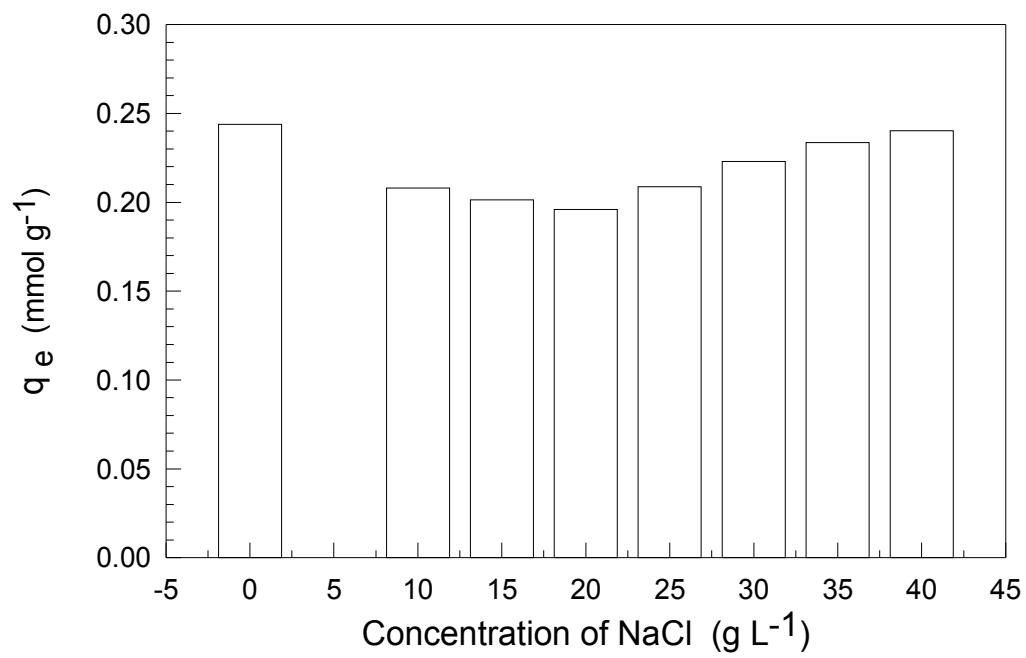


Fig. 7

**Fig. 8**